

Microfluidic Seeding of Cells on the Inner Surface of Alginate Hollow Microfibers

Saurabh S. Aykar, Nima Alimoradi, Mehrnoosh Taghavimehr, Reza Montazami, and Nicole N. Hashemi*

Mimicking microvascular tissue microenvironment *in vitro* calls for a cytocompatible technique of manufacturing biocompatible hollow microfibers suitable for cell-encapsulation/seeding in and around them. The techniques reported to date either have a limit on the microfiber dimensions or undergo a complex manufacturing process. Here, a microfluidic-based method for cell seeding inside alginate hollow microfibers is designed whereby mouse astrocytes (C8-D1A) are passively seeded on the inner surface of these hollow microfibers. Collagen I and poly-D-lysine, as cell attachment additives, are tested to assess cell adhesion and viability; the results are compared with nonadditive-based hollow microfibers (BARE). The BARE furnishes better cell attachment and higher cell viability immediately after manufacturing, and an increasing trend in the cell viability is observed between Day 0 and Day 2. Swelling analysis using percentage initial weight and width is performed on BARE microfibers furnishing a maximum of 124.1% and 106.1%, respectively. Degradation analysis using weight observed a 62% loss after 3 days, with 46% occurring in the first 12 h. In the frequency sweep test performed, the storage modulus (G') remains comparatively higher than the loss modulus (G'') in the frequency range 0–20 Hz, indicating high elastic behavior of the hollow microfibers.

1. Introduction


Microstructure scaffolds and hydrogels play a vital role in tissue engineering and regenerative medicine. Scaffolds provide a substrate for cell culture and proliferation to promote tissue

formation. One of the challenges in this field is to mimic the architecture of complex vascularized tissues.^[1] Microvessels are responsible for providing tissues with essential nutrients and oxygen while removing waste, hence mimicking these microvessels and studying their behavior is essential.^[2,3] In recent years, the fabrication of hydrogel-based microfibers that could mimic microvasculature systems has attracted many researchers in this area, and extensive research has been done to fabricate microfibers and to address cell encapsulation in these fibers.^[4,5,7–11] To improve the rheological and biological properties of microfibers, different organic and synthetic materials have been used for the fabrication of hydrogels and scaffolds; however, organic materials such as alginate-based microfibers showed better biocompatibility.^[4–6,12–14]

Different methods have been exploited to fabricate microfibers. Electrospinning has been widely used in the fabrication of micro/nanofibers.^[15] However, due to harsh fabrication process makes it an unsuitable environment for sensitive cell encapsulation. Moreover, poor mechanical properties and restrictions in the development of 3D structures are drawbacks that impede coculturing or multiple cell culturing that could mimic physiological functions of complex vascularized tissues.^[16] Microfluidic fabrication of these microstructures has attracted researchers in the field of tissue engineering and organ-on-chips.^[17–22] Microfluidic fabricated microfibers have made tremendous progress and can be used as scaffolds for different neural cells.^[19] Microfluidic devices are powerful tools for diverse biomedical engineering applications and are second to none in creating continuous biocompatible hydrogel microfibers with tightly controlled cross-section dimensions and shapes.^[20–26] Also, microfluidic methods provide a better environment for cell encapsulation, in terms of cell growth and proliferation, in comparison to the cell-electrospinning method. Also, fabricating a heterogeneous microfiber with different cell patterning is achievable by using a complex set of channels in a cell-friendly environment.^[14]

Cell encapsulation in microfiber is a novel technology that offers multiple applications in the area of tissue engineering. Hydrogel-based cell encapsulation is a highly efficient method that could improve in mimicking of tissues and provides

S. S. Aykar, N. Alimoradi, M. Taghavimehr, R. Montazami, N. N. Hashemi
Department of Mechanical Engineering
Iowa State University
Ames, IA 50011, USA
E-mail: nastaran@iastate.edu
N. N. Hashemi
Department of Mechanical Engineering
Stanford University
Stanford, CA 94305, USA

 The ORCID identification number(s) for the author(s) of this article can be found under <https://doi.org/10.1002/adhm.202102701>

© 2022 The Authors. Advanced Healthcare Materials published by Wiley-VCH GmbH. This is an open access article under the terms of the Creative Commons Attribution-NonCommercial License, which permits use, distribution and reproduction in any medium, provided the original work is properly cited and is not used for commercial purposes.

DOI: 10.1002/adhm.202102701

immunoisolation for cells.^[1,9,27–31] To simulate vascularized tissues, such as brain–blood barrier, having a cell lining on the inner surface of hollow microfibers is vital for its functionality. Seeding cells on the inner surface of the hollow microfiber is critical due to the adjacency of cells and the flow in the microfiber because cells are provided with more nutrients that are necessary for cell growth and proliferation.^[10,27] In our previous studies, cells were encapsulated in the wall and on the outer surface of the microfibers.^[5,27,29]

To this date, we know of no reports using a microfluidic chip to seed cells on the inner surface of hollow microfibers with capability of altering the dimension of hollow microfibers by merely changing the flow rates of different inlets while manufacturing. Moreover, this method gives the advantage of cell seeding on the inner surface and outer surface of the hollow microfiber as well as encapsulation of cells in the wall, simultaneously and without changing the setup. Additionally, this method does not require any post processing step once the cells are seeded on the inner layer of the hollow microfibers or encapsulated in the walls of hollow microfibers while manufacturing, which could preserve cell viability and growth. The main focus of this study was to use a microfluidic-based method to seed cells on the inner surface of the hollow microfiber while manufacturing and without any further postprocessing. Alginate was used for fiber fabrication as the sample solution, and polyethylene glycol (PEG) was used as core and sheath solution. Cells were mixed in the core solution that is used to shape the hollow part of the microfiber. To investigate the effects of different materials on cell attachment to the inner surface of the hollow microfiber, poly-D-lysine (PDL), and Collagen I (C1) were used as extracellular matrix (ECM), and results of which were compared to the non additive based (BARE) experiment. In addition, different flow rates were used to have different sizes of hollow alginate microfibers in terms of diameter. Mouse astrocyte cells were used in this study due to the high sensitivity of these cells to environmental parameters and have been monitored to determine the primary viability of cells with the suggested method for a course of 2 days. Also, the mechanical properties of the fabricated hollow microfibers were investigated in this study.

2. Results and Discussion

2.1. Manufacturing and Simultaneous Seeding of Cells on the Inner Surface of the Alginate Hollow Microfibers

Microfluidic devices manufactured by integrating the knowledge of engineering and biology have always been an essential tool in mimicking the microenvironment present at the cellular level in different mammalian organs or tissues for *in vitro* studies. We had previously developed a microfluidic chip that can be used to manufacture polyethylene glycol diacrylate (PEGDA) based hollow microfibers having an inner diameter less than 100 μm and were self-standing in nature.^[4] In this study, PEGDA was replaced by alginate as a substrate because it is an organic polymer obtained from marine brown algae, and when used as a scaffold, possesses one of the highest cell viabilities and an ability to crosslink into different shapes. Alginate hydrogel is a highly biocompatible and mechanically stable polymer that has been tested for various *in vitro* and *in vivo* applications.^[31–35] Moreover,

these hydrogels are also used as effective materials for many regenerative medicine applications such as wound healing because of their excellent water absorptivity, conformability, nontoxicity, and biodegradability.^[36–38] A similar microfluidic device was fabricated to manufacture alginate-based hollow fibers with altered dimensions to incorporate the considerably viscous alginate solution without clogging the microfluidic channels and, more particularly, the v-shaped grooves called chevrons. The chevrons were responsible for creating a concentric flow regime by utilizing the slightly protruded volume on all four sides of the microfluidic channel for the outer layer of fluid to advect on the top and bottom of the inner fluid stream. The mouse astrocytes (C8-D1A) cells were mixed with the core solution to eventually seed them on the inner surface of the hollow microfibers. After the polymeric solidification of the hollow microfibers, which is explained in detail in the Experimental Section and illustrated in **Figure 1**, the seeded cells in the hollow microfibers were stained using Invitrogen's live/dead cell assay to study the effect of the manufacturing process on the cell viability. Additionally, in an attempt to achieve maximum cell adhesion on the inner surface along with good cell viability, the two most common cell attachment factors, C1 and PDL were studied, and the results were compared with cell-seeded microfibers without any cell attachment additives (BARE). Moreover, different flow rate ratios (FRRs) were used to manufacture hollow microvessels allowing their use in different applications. The mouse astrocytes were used because they were readily available and are an integral part of the brain microvasculature, as the main goal was to demonstrate the microfluidic process of inner cell seeding that can mimic any microvasculature in the body.

2.2. Different Cell Attachment Factor Analysis

For cell seeding and attachment, two commonly used cell attachment additives, C1 and PDL were tested for cell viability during a short span (immediately and 1 day after manufacturing), and the results were compared with cell-seeded BARE microfibers. **Figure 2a–f** shows the live/dead fluorescence images of the mouse astrocyte cells that were seeded on the inner surface of the hollow microfibers containing either PDL, C1, or BARE as cell attachment additives. The cell viability was calculated using the live/dead cell fluorescence images captured on Day 0 (immediately after manufacturing) and Day 1 for PDL, C1, and BARE hollow microfibers and the average cell viabilities obtained were 87.55% and 91.14%, 77.05% and 84.58%, and 97.43% and 98.13%, respectively. **Figure 2g** shows the bar graph that compared the cell viabilities for both Day 0 and Day 1. The statistical significance analysis was performed using the ANOVA test followed by the Tukey's test (mean \pm standard deviation; $p < 0.05$ was used for significance analysis). A statistically significant difference was observed in the cell viability between BARE and C1, with the latter furnishing the lowest value. There was not any statistically significant difference observed between BARE and PDL; however, due to the cytotoxic attribute of the PDL residue within the microfiber, the use of the latter was neglected. Overall, an increasing trend was observed for all the microfibers between Day 0 and Day 1, with BARE having the highest, as evident from **Figure 2g**. The cell viability data for Day 0 were used to study

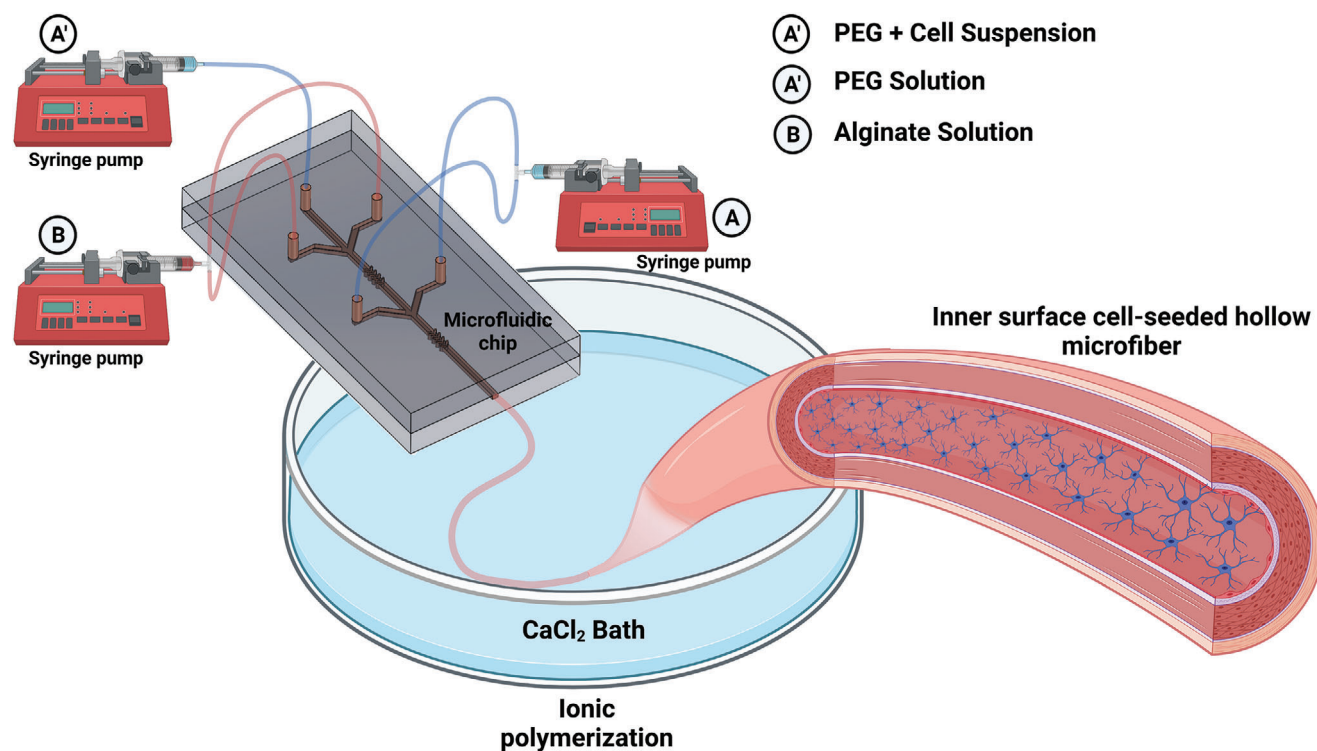


Figure 1. Schematic illustrating the microfluidic approach to manufacturing cell-seeded hollow microfibers. Mouse astrocyte (C8-D1A) cells were seeded on the inner surface of the alginate-based hollow microfibers using this method.

the exposure of cells to the polymer solutions and the imposed manufacturing effects. As evident from Figure 2a,c, there were some dead cells (red) observed in the microfibers with C1 and PDL on Day 0. For hollow microfibers with PDL as a cell attachment additive, the microfibers should be rinsed thoroughly with either maintenance media (MM) or phosphate buffered saline (PBS) to remove the excess PDL from the microfibers. The PDL could be cytotoxic even if a small amount of its residue remains in the microfibers. During manufacturing of cell-seeded hollow microfibers with C1 as cell attachment additive, inconsistent gelation of alginate and structural deformation were observed, leading to breakage of the microfibers along its length. However, for the BARE microfibers, a very low number of dead cells were observed as compared to PDL and C1, which is evident from Figure 2e. The higher cell viability in the case of BARE microfibers could be because of the direct binding sites provided on the innermost layer of the hollow microfibers by the gelation of alginate and equally due to the excellent cytocompatibility furnished by the alginate hydrogels. Moreover, a considerably higher number of cells were seeded with respect to the initial cell density of 2.6×10^6 cells mL^{-1} , indicating that the method is also efficient for seeding a lower number of cells. Moreover, the BARE microfibers possessed a desired hollow structure throughout its length during manufacturing. Since the BARE hollow microfibers exhibited good structural integrity, cell attachment and showed an increase in the cell viability for both days as opposed to PDL and C1, only BARE microfibers were used for further cell-seeding analysis.

2.3. Cell Viability Analysis for Cell-Seeded BARE Hollow Microfibers

Next, the cells were seeded on the inner surface of the BARE microfibers, and the cell viability was determined every 24 h for 2 days, as shown in Figure 3. The average cell viability on Day 0 was measured to be 97.43% which indicates that the manufacturing process did not impose adverse effects on the cell seeding process. Moreover, an increasing trend in the cell viability was observed during the course of the study from Day 0 to Day 2, indicating that the cells had enough exposure to MM throughout their growth. Additionally, it can be inferred that the porosity of the hollow microfibers allowed the diffusion of MM across the microfiber barrier to reach the internally seeded cells. To investigate the cell viability, the live/dead fluorescence images of the encapsulated cells were captured at different focal lengths along the width of the microfibers to image all the cells present. The high concentration (10×10^{-3} M) staining solution was used to stain the encapsulated cells for 45 min, which is the highest recommended time for staining as the staining solution should overcome the microfiber barrier. The z-stack of these images projected on a single plane, using ImageJ software, depicts that the cells were only seeded on the inner circumferential layer of the hollow microfibers as the cell count on the projected image was greater than any of the z-stack images. The good cell viability furnished shows that the inner surface of the hollow microfibers provided anchoring points for the cells to adhere and grow with abundant exposure to MM.

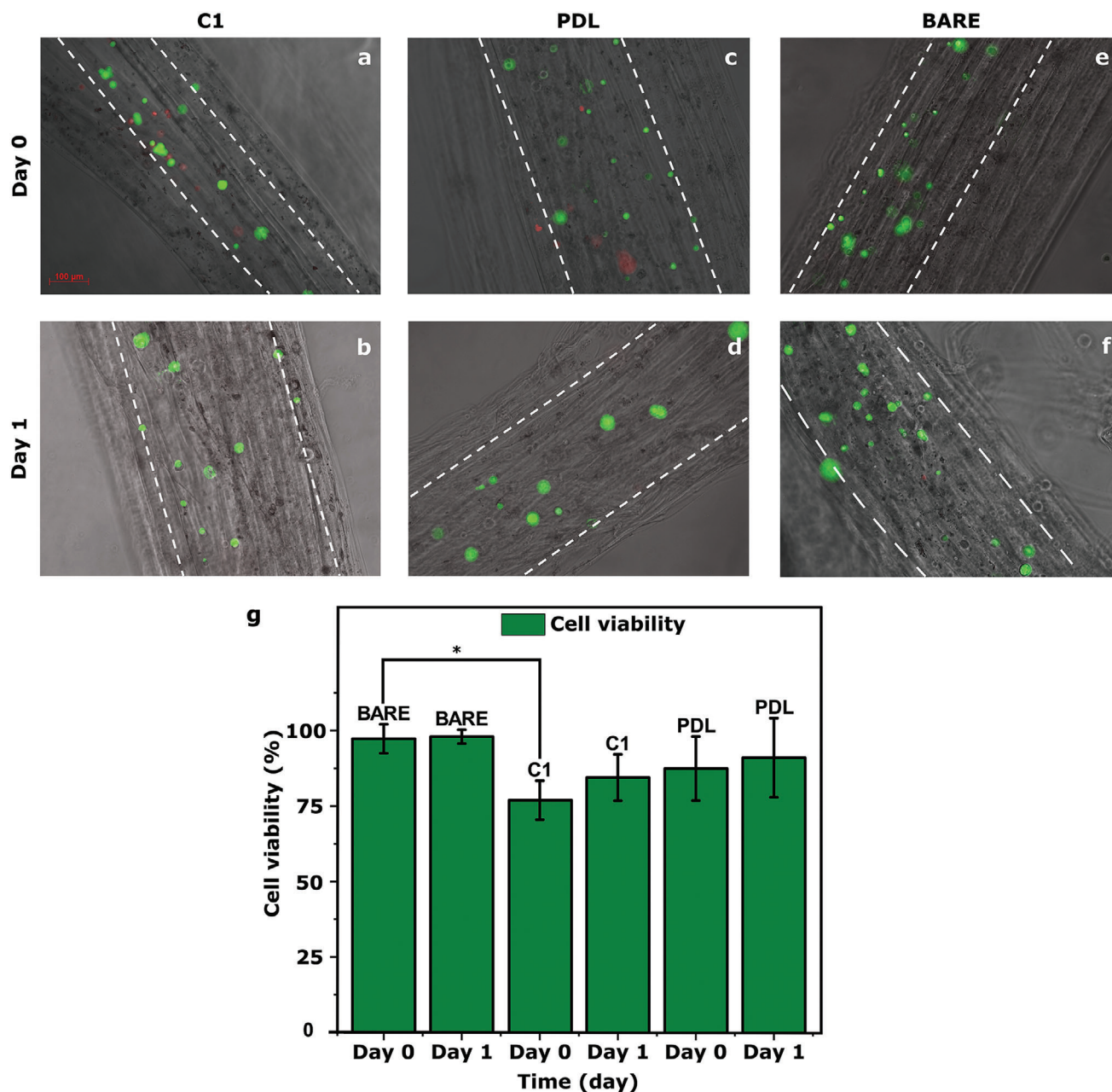


Figure 2. Comparison of the effect of different cell attachment additives with the bare one (without any cell attachment additives). a) Day 0 and b) Day 1 live/dead fluorescence images of the astrocyte cells seeded on the inner surface of the hollow microfibers using Collagen I (C1) as an ECM matrix, and c) Day 0 and d) Day 1 shows live/dead fluorescence images of the cells seeded on the inner surface of the hollow microfibers using poly-D-lysine (PDL) as an ECM matrix. e) Day 0 and f) Day 1 represent the live/dead fluorescence images of the astrocyte cells seeded hollow microfibers without any cell attachment additives (BARE). The scale bar is 100 μm . g) Cell viability was calculated using the live/dead cell fluorescence images and quantified as mean \pm standard deviation. For statistical significance analysis, ANOVA was performed followed by post hoc Tukey test; * $p < 0.05$ was used for statistical significance.

One of the advantages of this cell seeding technique is the exclusion of the use of any processing technique postmanufacturing the cell-seeded hollow microfibers. The microfiber manufacturing methods such as electrospinning, and direct extrusion by Ranjan et al. and Bosch-Rue et al., respectively, necessitates the additional postprocessing step of dissolving the centrally coaxial layer containing cells.^[9,10] Moreover, the hollow

microfibers fabricated using these techniques have a lower limit on the diameter of the fibers. However, our methodology of cell seeding incorporates the formation of the concentric fluid regime within the microfluidic chip, with cells present in the core solution, and instantly after polymerization, the template fluid runs into the bath solution through the microfiber barrier, leaving the cells trapped on their inner surface. Moreover,

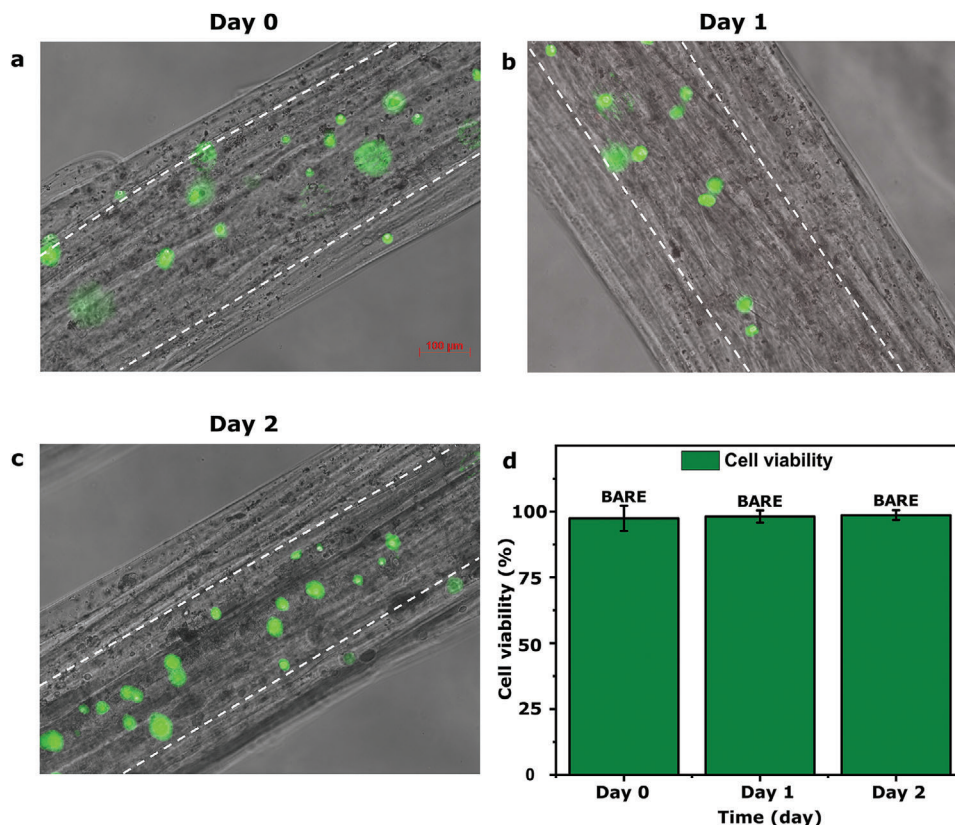


Figure 3. a–c) Live/dead cell assay images (Day 0 to Day 2) of the cells seeded on the inner surface of the alginate based hollow microfibers, without any ECM protein, simultaneously during manufacturing. Images depict the way mouse astrocytes were seeded on the inner surface of the hollow microfibers with a very few cells encapsulated in the walls. d) Bar graph indicating the increase in the cell viability from Day 0 to Day 2 for cells seeded in the BARE microfibers.

microfibers with variable diameters can be manufactured just by altering the FRRs of the input polymer solutions, SEM images of which are included in **Figure 4**.

2.4. Swelling and Degradation Analysis

The hollow microfibers manufactured were analyzed for their swelling properties when stored in the MM. They were assessed by measuring the weight and the width of the single strand of hollow microfiber every half hour for a total of 2 h and stored in the MM maintained at 37 °C and 5% CO₂ in the incubator. **Figure 5** shows the plots of the % initial weight and initial width of that microfiber measured over time. It was observed that the overall width of the hollow microfiber gradually increased by 6.1%, reaching its global maxima in the first 1 h and dropped by around 2.7% in the next hour. Similarly, the weight of the microfiber increased by 24.1% in the first half-hour and dropped by 13.9% in the next 1.5 h. The low swelling observed for the alginate microfibers could be attributed to their strong ionic crosslinking. The mimicking of any tissue or organ microenvironment largely depends on the swelling ability of the polymer used. Moreover, the swelling also depends on the degree of crosslinking of the alginate microfiber; highly crosslinked microfibers have limited swelling.

Next, to analyze the decreasing trend that was observed in both the weight and width of the microfibers after the initial increment, another experiment was performed to study the long-term effect. In this, the weight of the microfiber was measured every 12 h for a total of 72 h, the plot for which is shown in **Figure 5c**. The trend was only analyzed until 72 h of their storage, as after that, the handling and weighing process was hampered due to the breakage of the microfiber. A 46% sudden drop in the weight of microfiber was observed within the first 12 h justifying the fact that the alginate microfiber degrades in the MM over time.^[39,40] This degradation of the calcium crosslinked alginate microfibers could be the consequence of the exchange of crosslinked calcium ions with the MM. Moreover, the decreasing trend was observed to continue until 72 h, however with a considerable decrease in the rate of degradation. For a total of 3 days of incubation, the total weight of the microfiber decreased by 62%, with an initial drop of 46% in the first 12 h.

Next, the rheological measurements were studied by a frequency sweep test performed on a single strand of wet fiber. The storage modulus (G') and loss modulus (G'') were plotted, in **Figure 6**, over an oscillating frequency range of 0.02–20 Hz at 37 °C with a 0.25% initial strain. The G' measured remained higher than G'' over the studied range of frequency which indicates that the microfiber showed high elastic behavior, compared to the viscous one. This also indicates that strong ionic crosslinking

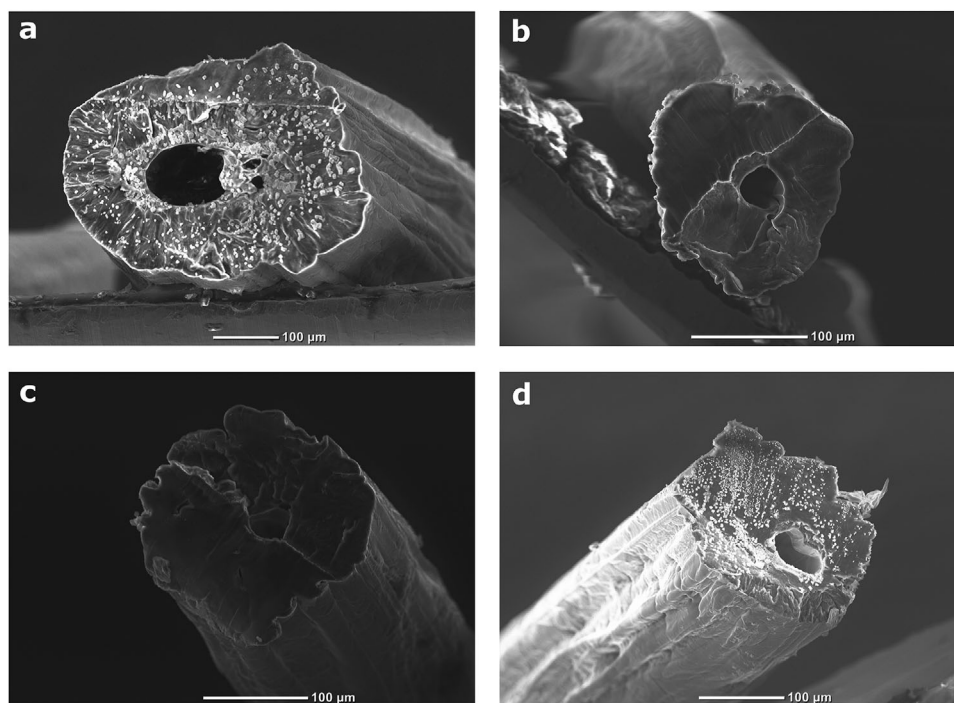


Figure 4. Scanning electron microscope (SEM) images of the alginate-based hollow microfibers manufactured using different flow rate ratios (FRRs): a) 600:250:200 $\mu\text{L min}^{-1}$, b) 200:100:400 $\mu\text{L min}^{-1}$, c) 200:100:500 $\mu\text{L min}^{-1}$, and d) 100:100:200 $\mu\text{L min}^{-1}$. The scale bar is 100 μm .

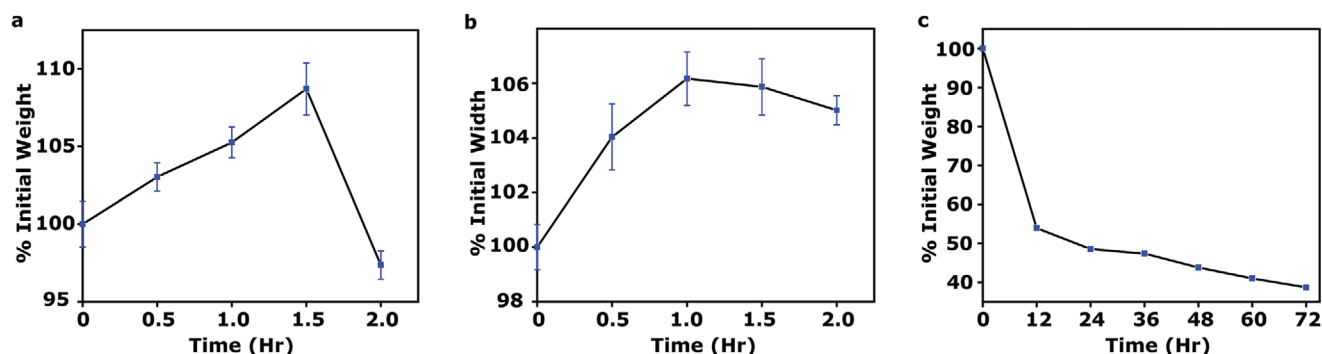


Figure 5. Swelling and degradation analysis of the alginate-based hollow microfibers stored in maintenance media (MM) maintained at 37 °C and 5% CO_2 . For swelling analysis, the weight a) and width b) of the microfiber are measured every half hour for a total of 2 h, results of which are plotted as % initial quantity every half hour and the error bars equal 1 standard deviation. Similarly, the degradation analysis was performed by measuring weight c) every 12 h for a total of 72 h, and the result was plotted as % initial quantity. The error bar equals one standard deviation.

bonds were formed between alginate and calcium ions that subsequently restricted the swelling of the microfibers, as observed in this study. A 3.5% w/v concentration of alginate solution was selected because of its potential to form hydrogels with higher mechanical stiffness.^[41] In general, it was crucial to analyze the mechanical properties of these hollow microfibers as they greatly affect the cell–substrate interaction.

3. Conclusion

In conclusion, a microfluidic approach was designed to seed mouse astrocyte cells on the inner surface of the hollow microfibers during manufacturing. Cell attachment on the inner

surface was studied using C1 and PDL; the results were compared with the BARE ones manufactured without any cell attachment additives. The results suggest that the BARE hollow microfibers potentially exhibited effective cell attachment and better cell viability immediately after manufacturing (Day 0 and Day 1) and were used for further analysis. The BARE microfibers furnished high cell viability immediately (Day 0) and throughout the observation period (until Day 2), which indicates that the microfluidic approach of cell seeding had minimal effect on the cell viability. Subsequently, swelling of the BARE microfibers was studied using their weight and width, and the findings indicate that limited swelling was observed, which can be attributed to higher crosslinking between alginate

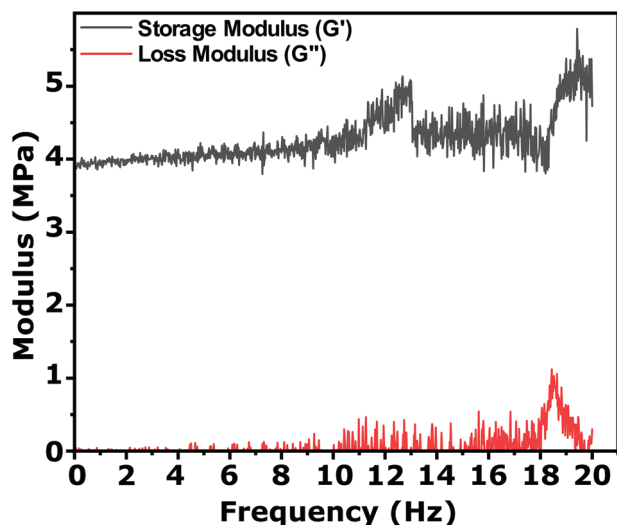


Figure 6. The graph shows the result of the frequency sweep test performed on the alginate-based hollow microfiber. The storage modulus (G') represents the elastic behavior of microfiber whereas, the loss modulus (G'') represents the viscous behavior. In the frequency range 0–20 Hz, the G' is considerably higher than the G'' indicating the elastic behavior of the microfiber within the operated frequency range.

and calcium ions. Lastly, the rheological measurement using frequency sweep test was performed on the BARE microfiber, which indicated that it possessed exceptionally higher elastic modulus compared to viscous modulus. Overall, this simplistic microfluidic approach enables inner surface cell seeding in alginate-based hollow microfibers, with minimal effect on the cell viability, with a potential to accelerate its use in mimicking several microvascular microenvironments in vitro.

4. Experimental Section

Materials: Polymethyl methacrylate (PMMA), commonly known as Acrylic, sheets with 6 mm thickness were used as a substrate for the fabrication of the microfluidic device. A flat bottom AlTiN-coated end-mill having a diameter of 0.2 mm, that was used to mill the microfluidic design onto the PMMA sheets was purchased from Grainger (Lake Forest, IL, USA). PEG ($M_w = 20\,000$ Da) was purchased from Sigma-Aldrich (St. Louis, MO, USA), and Calcium Chloride Dihydrate ($\text{CaCl}_2 \cdot 2\text{H}_2\text{O}$) was purchased from Thermo Fisher Scientific (Waltham, MA, USA), Sodium Alginate salt was purchased from AlphaAesar (Tewksbury, MA, USA). Deionized (DI) water was obtained from a Thermo Fisher Scientific DI water system (Waltham, MA, USA). PDL was purchased from MilliporeSigma (Burlington, MA, USA), and C1 was from Corning (Glendale, Arizona, USA).

Microfluidic Chip Fabrication: The fabrication of the microfluidic chip is explained in detail in the previous article.^[4] Briefly, the microfluidic design consists of a core microfluidic channel that runs along the length of the chip and has a dimension of $1\text{ mm} \times 0.75\text{ mm}$ (width \times height), a pair of a set of chevrons having dimensions $0.8\text{ mm} \times 0.625\text{ mm}$ (width \times height) with each set having four chevrons, and three inlets for flowing distinct polymer solutions. The microfluidic design is divided into two equal halves along its height and is micromilled onto two polymethyl methacrylate (PMMA) chips. Subsequently, these two PMMA chips are bonded together using a solvent-assisted bonding technique to form a hollow microvessel producing microfluidic device.^[27]

Cell Culture: C8-D1A (ATCC, Manassas, VA, USA) cells were used for seeding on the inner surface of the hollow microfibers. The cells were cultured in a T-25 flask (Thermo Fisher Scientific, Waltham, MA, USA) containing MM, and were stored in an incubator maintained at 37°C and 5% CO_2 until 90% confluency was achieved. The MM was prepared by mixing 90% Dilbecco's modified Eagle's medium (DMEM) (Lonza, Waltham, MA, USA) with 10% qualified one-shot Fetal Bovine Serum (Gibco, Waltham, MA, USA), which was supplemented with 1% penicillin ($10\,000\text{ U mL}^{-1}$)–streptomycin ($10\,000\text{ }\mu\text{g mL}^{-1}$) (Gibco, Waltham, MA, USA). The cells were then passaged and suspended in 1 mL MM to a final density of 2.6×10^6 cells mL^{-1} .

Concentric Fluid Regime Formulation: Two polymer solutions, namely PEG and Alginate (precursor), were used in developing the concentric fluid regime within the microfluidic device that eventually undergoes ionic polymerization to form hollow alginate microfibers. The PEG solution was introduced as a template fluid through a core inlet and a pair of sheath inlets, whereas the precursor alginate was made to flow through a pair of cladding inlets. The core inlet directly connects the central channel, following which the pair of cladding and sheath inlets merges from either side onto the central channel in the order mentioned. Two sets of chevrons, a set consisting of four chevrons each, were milled on the central channel with one set located in between the pair of cladding and sheath inlets while another present in between the pair of cladding inlets and the outlet of the device. After the introduction of PEG solution through the core inlet in the central channel, it is compressed laterally by the alginate solution at the first hydrodynamic focusing region. At this point, the laterally compressed fluid regime spans the vertical height of the central channel, with alginate solution being on either side of the PEG solution. This particular fluid regime travels through the set of four chevrons where the outer solution (alginate) advects on the top and bottom of the inner solution (PEG). The advection occurs due to the extra volume provided by the chevrons on all sides of the central channel. After the concentric fluid regime developed with PEG being engulfed by the alginate solution, it passes through the second hydrodynamic region where the PEG enters through the pair of cladding inlets. Similar vertical spanning occurs with PEG being the outer fluid compressing the already developed concentric fluid regime. Subsequently, the PEG advects on the top and bottom after passing through the second set of chevrons and engulfs the concentric fluid regime. Ultimately, a three-layer concentric fluid regime is developed at the end of the microfluidic channel with PEG on the inner and outer layer while alginate is present in between. The step-by-step formulation of the cross-section of the fluid regime developed at five distinct points along the central channel is depicted in Figure S3 (Supporting Information). As this fluid regime comes in contact with the CaCl_2 solution, the alginate layer polymerizes to form a hollow tube while the template fluid PEG runs into the water bath.

Inner Surface Cell Seeding and Manufacturing of Hollow Microfibers: The microfluidic device was rinsed by first flowing 70% v/v ethanol following PBS, each for 30 min, to achieve sterilization. Moreover, it was then exposed to ultraviolet (UV) light under a biosafety level 2 cabinet for additional 25 min. Since the glass transition temperature of PMMA is 110°C , the autoclave was not chosen as a sterilization method. The core and sheath solutions were prepared by mixing 30 wt% PEG with DI water. Similarly, the cladding solution was prepared by mixing 3.5 wt% alginate with DI water and the collection bath solution by mixing 15 wt% CaCl_2 in DI water. All solutions were mixed using a magnetic stirrer for 24 h until homogenous and were then autoclaved to ensure sterility.

Three types of hollow fibers were manufactured with two different ECM proteins, namely poly-D-lysine and Collagen I and one without any ECM protein, for which different core solutions were used. The core solution consisted of 30 wt% PEG in DI water for fibers manufactured without any ECM matrix; it was additionally mixed with 0.01 wt% PDL or 0.01 wt% C1 for PDL or C1 fibers, respectively. Approximately, 2.6×10^6 cells in 1 mL MM were mixed with 1 mL core solution containing PEG. This mixture was made to flow through the core inlet using a syringe pump in infusion mode. The alginate solution was then pumped through the cladding and the PEG solution (without cells) through the sheath inlets simultaneously. The FRR used to pump these fluids was chosen to be 600:250:200 (core:cladding:sheath). A concentric flow regime was

developed at the outlet of the microfluidic device that flows into the bath solution. As the Alginate layer from the developed concentric fluid regime comes in contact with the CaCl_2 in the bath solution, due to ionic crosslinking between alginate and calcium ions, the alginate solidifies, forming a hollow microfiber while the cells in the core solution attach to the inner surface of the crosslinked hollow fiber and the PEG solutions simply run into the bath solution. The cell-seeded hollow microfibers were transferred to a 6-well culture plate containing MM, and it was changed every 24 h for them to have a continuous supply of nutrients and vitamins for cell maintenance and proliferation.

Cell Viability Determination: At desired time points, the MM was aspirated from one of the 6-well plates containing the cell-seeded microfibers. The cell staining solution was prepared by mixing Invitrogen's CMFDA Green (10×10^{-3} M) and Propidium Iodide (10×10^{-3} M) in base media for staining live cells and dead cells, respectively. The high concentration (10×10^{-3} M) was used to penetrate and overcome the barrier provided by the alginate microfibers as the cells were seeded on their inner surface. 2 mL staining solution was used to stain the microfibers per well. The wells were incubated at 37 °C for 45 min. Subsequently, the staining solution was aspirated, and the wells were washed with PBS before adding the MM. The wells were then imaged for live/dead cell fluorescence using an inverted microscope.

Swelling and Degradation Analysis: The swelling of the hollow microfibers was studied by measuring their width and weight. A single microfiber manufactured (without cells) with FRR 600:250:200 $\mu\text{L min}^{-1}$ was completely submerged in the MM and stored in the incubator maintained at 37 °C and 5% CO_2 . It was weighed and imaged using an inverted optical microscope every half-hour for a total of 2 h. Similarly, for the alginate degradation analysis in the MM, another single microfiber was weighed every 12 h for a total of 72 h.

Rheological Analysis: The investigation of the mechanical properties of the alginate-based hollow microfibers was performed by measuring their rheological parameters using Dynamic Mechanical Analyzer (DMA) (Mettler Toledo, Columbus, OH, USA). The noncell-seeded hollow microfiber, immediately after manufacturing, was mounted on the DMA, and a frequency sweep test, having a frequency range of 0.02–20 Hz, was performed to determine its viscoelastic properties, G' , and G'' . G' indicates the microfiber's elastic property, whereas the G'' exhibits the viscous property.

SEM Imaging: For imaging, the alginate-based hollow fibers were manufactured without the incorporation of cells. After manufacturing these hollow microfibers, they were wrapped on a cardboard mount, as shown in Figure S1b (Supporting Information), and were allowed to dry overnight at ambient temperature. Once dried, the fibers were cut into small fragments along their length and were mounted vertically on a 3M copper electrical tape (3M, Saint Paul, MN, USA), as depicted in Figure S1c (Supporting Information). The microfibers mounted copper tape was inserted into a JOEL JCM-6000 Benchtop SEM, which was used to capture the images of the cross-sectional view of the hollow microfibers as shown in Figure 4.

Statistical Analysis: Statistical analysis for significance was performed on R and RStudio for all the cell viability calculations using ANOVA test followed by post hoc Tukey test, $*p < 0.05$.

Supporting Information

Supporting Information is available from the Wiley Online Library or from the author.

Acknowledgements

This work was partially supported by the Office of Naval Research (ONR) Grant N000141712620 and National Science Foundation Award 2014346. Open access funding provided by the Iowa State University Library.

Conflict of Interest

The authors declare no conflict of interest.

Data Availability Statement

The data that support the findings of this study are available from the corresponding author upon reasonable request.

Keywords

biopolymers, cell seeding, hollow microfibers, microfluidics, microvascular tissues

Received: December 10, 2021

Published online:

- [1] A. Khademhosseini, R. Langer, *Biomaterials* **2007**, *28*, 5087.
- [2] R. Daneman, A. Prat, *Perspect. Biol.* **2015**, *7*, a020412.
- [3] M. S. Alavijeh, M. Chishty, M. Z. Qaiser, A. M. Palmer, *NeuroRx* **2005**, *2*, 554.
- [4] S. S. Aykar, D. E. Reynolds, M. C. McNamara, N. N. Hashemi, *RSC Adv.* **2020**, *10*, 4095.
- [5] F. Sharifi, B. B. Patel, M. C. McNamara, P. J. Meis, M. N. Roghair, M. Lu, R. Montazami, D. S. Sakaguchi, N. N. Hashemi, *ACS Appl. Mater. Interfaces* **2019**, *11*, 18797.
- [6] H. Acar, S. Cinar, M. Thunga, M. R. Kessler, N. Hashemi, R. Montazami, *Adv. Healthcare Mater.* **2014**, *24*, 201304186.
- [7] S. K. Chae, E. Kang, A. Khademhosseini, S. H. Lee, *Adv. Mater.* **2013**, *25*, 3071.
- [8] Z. Bai, J. M. M. Reyes, R. Montazami, N. Hashemi, *J. Mater. Chem. A* **2014**, *2*, 4878.
- [9] V. D. Ranjan, P. Zeng, B. Li, Y. Zhang, *Biomater. Sci.* **2020**, *8*, 2175.
- [10] E. Bosch-Ru e, L. M. Delgado, F. J. Gil, R. A. Perez, *Biofabrication* **2020**, *13*, 015003.
- [11] S. Barroso-Solares, D. Cuadra-Rodr guez, M. L. Rodr guez-Mendez, M. A. Rodr guez-Perez, J. Pinto, *J. Mater. Chem. B* **2020**, *8*, 8820.
- [12] K. Wang, J. Guan, F. Mi, J. Chen, H. Yin, J. Wang, Q. Yu, *Mater. Lett.* **2015**, *161*, 317.
- [13] J. Stephens-Altus, P. Sundelacruz, M. Rowland, J. West, *J. Biomed. Mater. Res., Part A* **2011**, *98*, 167.
- [14] B. Lu, M. Li, Y. Fang, Z. Liu, T. Zhang, Z. Xiong, *Front. Bioeng. Biotechnol.* **2020**, *8*, 610249.
- [15] J. Cheng, Y. Jun, J. Qin, S.-H. Lee, *Biomaterials* **2017**, *114*, 121.
- [16] J. Hong, M. Yeo, G. H. Yang, G. Kim, *Int. J. Mol. Sci.* **2019**, *20*, 6208.
- [17] G. A. Clarke, B. X. Hartse, A. E. Niaraki Asli, M. Taghavimehr, N. Hashemi, M. Abbasi Shirsavar, R. Montazami, N. Alimoradi, V. Nasirian, L. J. Quedraogo, N. N. Hashemi, *Sensors* **2021**, *21*, 1367.
- [18] M. C. McNamara, S. S. Aykar, N. Alimoradi, A. E. Niaraki Asli, R. L. Pemathilaka, A. H. Wrede, R. Montazami, N. N. Hashemi, *Adv. Biol.* **2021**, *5*, 2101026.
- [19] B. Buchroithner, S. Mayr, F. Hauser, E. Priglinger, H. Stangl, A. R. Santa-Maria, M. A. Deli, A. Der, T. A. Klar, M. Axmann, *ACS Nano* **2021**, *15*, 2984.
- [20] D. Sechi, B. Greer, J. Johnson, N. Hashemi, *Anal. Chem.* **2013**, *85*, 10733.
- [21] J. D. Caplin, N. G. Granados, M. R. James, R. Montazami, N. Hashemi, *Adv. Healthcare Mater.* **2015**, *4*, 1426.
- [22] R. L. Pemathilaka, D. E. Reynolds, N. N. Hashemi, *Interface Focus* **2019**, *9*, 20190031.
- [23] R. L. Pemathilaka, J. D. Caplin, S. S. Aykar, R. Montazami, N. N. Hashemi, *Global Challenges* **2019**, *3*, 1800112.
- [24] N. Hashemi, J. M. Lackore, F. Sharifi, P. J. Goodrich, M. L. Winchell, N. Hashemi, *Technology* **2016**, *4*, 98.
- [25] B. Chen, F. Tian, N. Hashemi, M. McNamara, M. Cho, *J. Mater. Sci. Eng.* **2018**, *7*, 2169.

- [26] R. Booth, H. Kim, *Lab Chip* **2012**, *12*, 1784.
- [27] M. C. McNamara, S. S. Aykar, R. Montazami, N. N. Hashemi, *ACS Macro Lett.* **2021**, *10*, 732.
- [28] S. I. Ahn, Y. J. Sei, H.-J. Park, J. Kim, Y. Ryu, J. J. Choi, H.-J. Sung, T. J. MacDonald, A. I. Levey, Y. Kim, *Nat. Commun.* **2020**, *11*, 175.
- [29] F. Sharifi, B. B. Patel, A. K. Dzuilko, R. Montazami, D. S. Sakaguchi, N. Hashemi, *Biomacromolecules* **2016**, *17*, 3287.
- [30] A. Bamshad, A. Nikfarjam, H. Khaleghi, *J. Micromech. Microeng.* **2016**, *26*, 065017.
- [31] T. A. Becker, D. R. Kipke, T. Brandon, *J. Biomed. Mater. Res.* **2001**, *54*, 76.
- [32] K. Y. Lee, D. J. Mooney, *Prog. Polym. Sci.* **2012**, *37*, 106.
- [33] U. Rottensteiner, B. Sarker, D. Heusinger, D. Dafinova, S. N. Rath, J. P. Beier, U. Kneser, R. E. Horch, R. Detsch, A. R. Boccaccini, *Materials* **2014**, *7*, 1957.
- [34] J. B. De Souza, G. d. S. Rosa, M. C. Rossi, F. d. C. Stievani, J. P. H. Pfeifer, A. M. T. Kriek, A. L. d. C. Bovolato, C. E. Fonseca-Alves, V. A. Borrás, A. L. G. Alves, *Front. Bioeng. Biotechnol.* **2021**, *9*, 674581.
- [35] F. Abasalizadeh, S. V. Moghaddam, E. Alizadeh, E. akbari, E. Kashani, S. M. B. Fazljou, M. Torbati, A. Akbarzadeh, *J. Biol. Eng.* **2020**, *14*, 8.
- [36] J. Sun, H. Tan, *Materials* **2013**, *6*, 1285.
- [37] M. Zhang, X. Zhao, *Int. J. Biol. Macromol.* **2020**.
- [38] M. Salehi, A. Ehterami, S. Farzamfar, A. Vaez, S. Ebrahimi-Barough, *Drug Delivery Transl. Res.* **2021**, *11*, 142.
- [39] N. C. Hunt, R. M. Shelton, D. J. Henderson, L. M. Grover, *Tissue Eng., Part A* **2013**, *19*, 905.
- [40] M. S. Shoichet, R. H. Li, M. L. White, S. R. Winn, *Biotechnol. Bioeng.* **1996**, *50*, 374.
- [41] P. Duan, N. Kandemir, J. Wang, J. Chen, *MRS Adv.* **2017**, *2*, 1309.